metals

MDPI

Article

The Influence of Multi-Pass Friction Stir Processing on the Microstructure Evolution and Mechanical Properties of IS2062 Steel

Avinash Ravi Raja, Hao Su and Chuansong Wu *

Institute of Materials Joining, Shandong University, Jinan 250061, China; avinash.raja@sdu.edu.cn (A.R.R.); suh@email.sdu.edu.cn (H.S.)
* Correspondence: wucs@sdu.edu.cn

Abstract: The motive of present work is to explore the variation in the material characteristics of steel upon multi-pass friction stir processing. Steel plates (IS2062) that were 3 mm thick, were subjected to friction stir processing in a multi-pass manner. The selected transverse speed was 150 mm/min, along with a tool rotation of 800 RPM when using a tungsten carbide tool (shoulder diameter—10 mm). Steel plates were processed using the single-pass, double-pass, and triple-pass travel of the rotating tool to observe the impact of multi-pass processing on the properties of steel plates. Multi-pass friction stir processing resulted in a higher micro-hardness of 175 VHN after the second pass, in comparison to the unprocessed metal, which had a micro-hardness of 130 VHN, owing to the collective effect of the plastic flow of the material due to the rotation of the tool and frictional heat, which also leads to grain refinement. The second pass evidenced an average grain size of 22 microns, whereas the unprocessed material had an average grain size of 57 microns. The results of EBSD and SEM characterization showed reasonably improved material properties of the processed work materials.

Keywords: multi-pass friction stir processing; EBSD; SEM; grain refinement

check for updates

Citation: Raja, A.R.; Su, H.; Wu, C. The Influence of Multi-Pass Friction Stir Processing on the Microstructure Evolution and Mechanical Properties of IS2062 Steel. *Metals* **2024**, *14*, 685. https://doi.org/10.3390/met14060685

Academic Editor: Masahiro Fukumoto

Received: 30 April 2024
Revised: 31 May 2024
Accepted: 6 June 2024
Published: 9 June 2024

Copyright: © 2024 by the authors. Licensee MDPI, Basel, Switzerland. This article is an open access article distributed under the terms and conditions of the Creative Commons Attribution (CC BY) license (https://creativecommons.org/licenses/by/4.0/).

1. Introduction

Due to its versatility, durability, strength, and cost-effectiveness, IS2062 steel has been the preferred choice for a broad range of applications across various industries, including the construction of bridges, buildings, transmission towers, and industrial structures. Since the call for advanced structural steels continues to increase as construction practices evolve, the industry seeks new materials or the advancement of existing materials in order to offer a superior performance, sustainability, cost efficiency, and design flexibility. Among several techniques to advance existing materials, friction stir processing (FSP), invented by Mishra et al., offers a promising approach to tailor the microstructure and properties of structural steel for various applications, providing opportunities to enhance its performance and extend the material's capabilities beyond the conventional limits [1]. FSP is a fascinating technique that has collected weighty attention due to its ability to modify the microstructure and properties of work materials. FSP is a solid-state material processing method that improves the properties of metals below the melting temperature of the materials. Friction stir processing (FSP) evolved from friction stir welding (FSW) technology, which also comprises similar principles. During FSP, a non-consumable rotating tool with a pin and a shoulder is used to process a single piece of material, resulting in specific property enhancements [2–4]. The shoulder generates heat, because of friction, to plasticize the material, while the rotating tool pin inside the material causes the flow of material under elevated temperature conditions [5–8]. This frictional heat causes the flow of work-piece material around the tool periphery [9]. The friction between the rotating tool shoulder and the work-piece also generates heat, which is further transferred to the work-piece. The flow of work material in the plastic stage under the action of a rotating pin and elevated

temperature conditions due to frictional heat leads to grain refinement [10–14], which causes an increase in hardness [15]. The depth of the penetration of the tool pin [16] into the work-piece is maintained, so as to ensure the appropriate contact between the work-piece surface and the tool shoulder. Friction stir processing is becoming a popular manufacturing process for surface modification with enhancements in mechanical properties [17–20].

FSP can also modify the surface layer by introducing reinforcing particles or other materials [21]. The material undergoes hardening due to deformation and recrystallization processes. FSP allows for the fabrication of hybrid and in situ surfaces with tailored properties. While FSP has been extensively studied in non-ferrous metal alloys (such as aluminum, copper, titanium, and magnesium), the implementation of FSP on steel is also relevant [22–25]. Steel components in various industries (e.g., aerospace, automotive, and construction) can benefit from FSP [26,27]. Experimental data reveal changes in the microstructure, mechanical properties, and tribological behavior of steel alloys processed using FSP [28–30]. FSP allows for the customization of material properties based on specific requirements. Fine-grained microstructures enhance the toughness and flexibility of the material. Unlike traditional welding, FSP is a solid-state process, minimizing distortion and avoiding melting.

Han et al. [31] studied the microstructure evolution, mechanical enhancement, and texture modification of friction stir-processed Mg-14Gd alloys and observed a significant grain refinement upon friction stir processing. Orozco-Caballero et al. [32] severely friction stir processed an over-aged Al 7075 alloy at various severity conditions obtained by changing the rotational speed and the traverse speed, and observed a wide variety of very-fine grain sizes and misorientations. They also found a relation between mean misorientations and grain size. Miles et al. [33] advocated friction stir processing for the repair of stainless steel reactor components manufactured using conventional fusion welding in the nuclear industry. The conventional fusion welding process results in the development of intergranular cracks in the heat affected zone; on the other hand, friction stir processing may be employed as a crack repair method as it generates a lower peak temperature than fusion welding. In a recent study, Selvam et al. [34] demonstrated a novel application of submerged friction stir processing to control the cavitation erosion–corrosion by tailoring the surface properties to generate tailored microstructures.

Multiple processing passes in FSP are very effective in improving the surface properties of the material, which extends the domains of application areas of that particular material. The majority of previous researchers engaged in the area of friction stir welding have used this technique for the joining of materials such as aluminum and its alloys, which plasticize at a lower temperature; only a few researchers have attempted the FSW technique on steel as it is difficult to process using FSW, due to its increased hardness value and the requirement of a higher temperature to plasticize the steel [35]. A critical literature review reveals that less work has been reported on the in-depth characterization of multi-pass-processed steel. Hence, the objective of the present experimental work is to study the effect of the multi-pass friction stir processing of steel on the material properties of IS2062 steel.

2. Materials and Methods

An IS2062 GR B structural steel plate of 3 mm thickness was selected for the current study and was procured from a local supplier. The elemental composition of the as-received mild steel sample was analyzed using energy-dispersive X-ray spectroscopy (EDX) and is shown in Table 1. To study the effect of the number of passes on the degree of grain refinement, multi pass friction stir processing was performed using a numeric-controlled FSW machine (Supplied by RV Machine Tools, Coimbatore, India) with a 3 Ton capacity on mild steel plates; three samples were prepared, with a different number of passes (single pass, double pass, and triple pass). A commercial tungsten carbide tool, with a conical pin length of 2.2 mm and a shoulder diameter of 10 mm, as shown in Figure 1, was employed for processing. A tool tilt angle of 1.5° was provided for defect-free welding. The steel plates were friction stir processed using a tungsten carbide tool at a welding speed of 150

mm per minute and a spindle revolution of 800 RPM. The optimized parameters of FSP were chosen for this study after several pilot experiments.

Table 1. Chemical composition (wt. %) of base material.

C	Si	Mn	P	S	Cr	Fe
0.21	0.45	1.37	0.04	0.04	0.11	Bal.

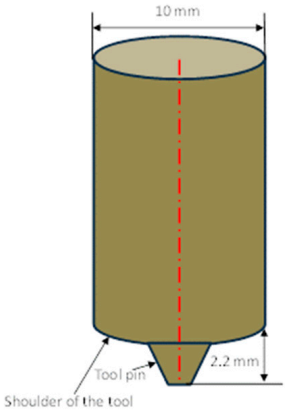

Figure 1. Schematic diagram of tungsten carbide (WC) tool.

Surface modification by varying the number of passes through friction stir processing has been carried out, as is shown schematically in Figure 2, where the red one indicates the single pass (sp), green is used for the double pass (dp) and the purple is used to show the third pass (tp). After the processing, samples of the required size were cut from the base metal and processed metal for microhardness testing, as well as for metallographic analysis. Before the examination, all the samples were polished using emery paper and alumina paste, following the standard procedure. Surface and cross-sectional micrographs were captured using an optical microscope after etching with a solution of nitric acid (5% Nital). The microhardness testing of the samples was performed using Vickers microhardness testing machine (Supplied by Conation, Pune, India) under an applied load of 200 g for 10 s of dwell time. The tensile test specimens were extracted from the center of the processed sample and were machined as per the ASTM E-8 standard [36].

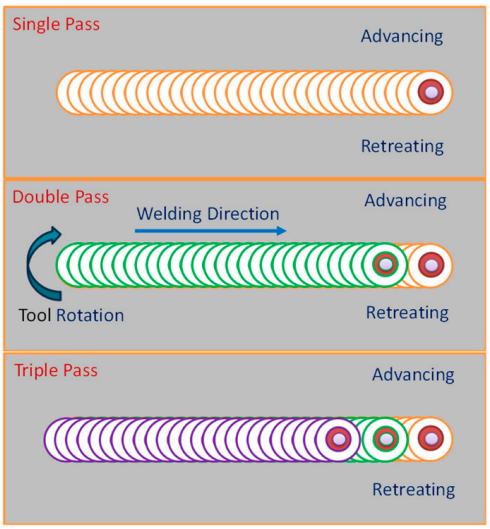

Figure 2. Schematic representation of friction stir-processed samples after single, double, and triple passes.

3. Results

The metallographic analysis of the friction stir-processed samples was carried out using a stereo microscope. Figure 3 represents the macro-view of the cross-section of the friction stir-processed samples after a single pass, a double pass, and a triple pass to show the flow of the materials in the processed zone.

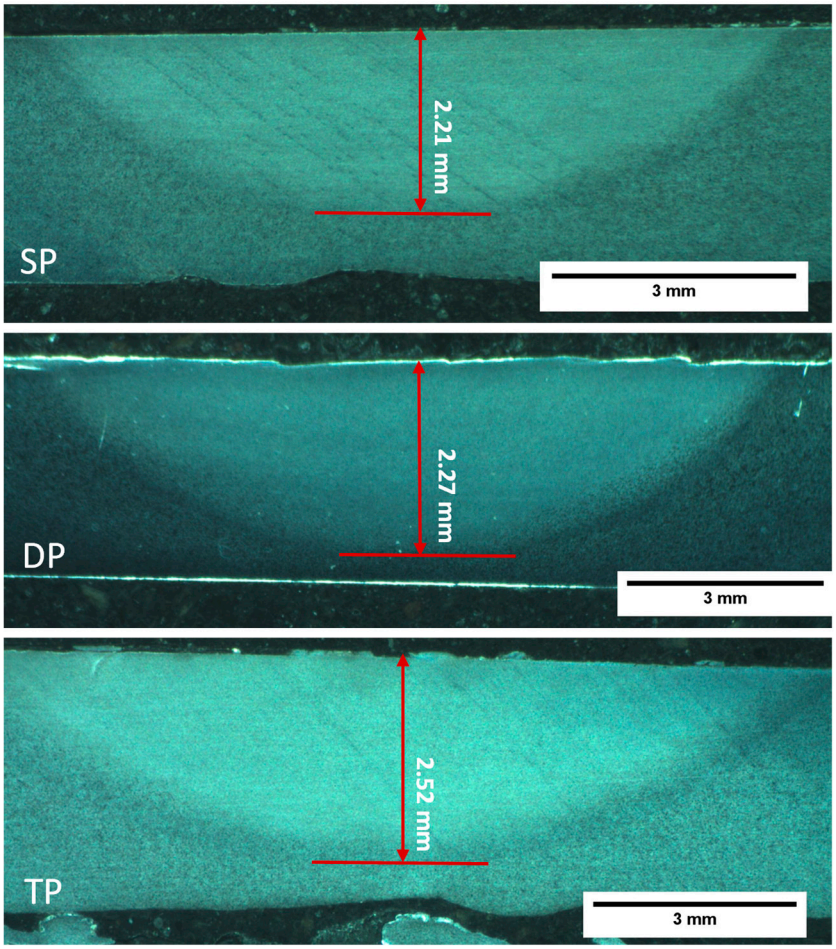

Figure 3. Optical macrograph of the cross-section of the friction stir-processed samples after single, double, and triple passes.

The microstructure of the base material, as well as after three sequential passes, is shown in Figure 4. It can clearly be seen that friction stir processing caused grain refinement in the processed region due to the stirring of the material around the periphery of the pin, as well as the frictional heat input under the controlled load. The linear intercept method was used to evaluate the average grain size for all the samples and the results are listed in Figure 5.

Microhardness results was shown in Figure 6 whereas the ultimate tensile strength (UTS) was evaluated and is shown in Figure 7 for all the processed samples after smoothing the gauge area with the help of 100 grit emery paper. All the tensile test specimens were prepared as per the standard of the ASTM, using wire-cut EDM.

A scanning electron microscope was also used to characterized the friction stir processed samples with different magnifications. The SEM results of the triple pass-processed sample clearly reveal the fine lamellae of the pearlites colony, as shown in Figure 8, whereas the as-received material has equiaxed ferrite grains of approximately 35 to 50 μm in diameter, as shown in Figures 4 and 6. The double pass sample has a dense distribution of the pearlites.

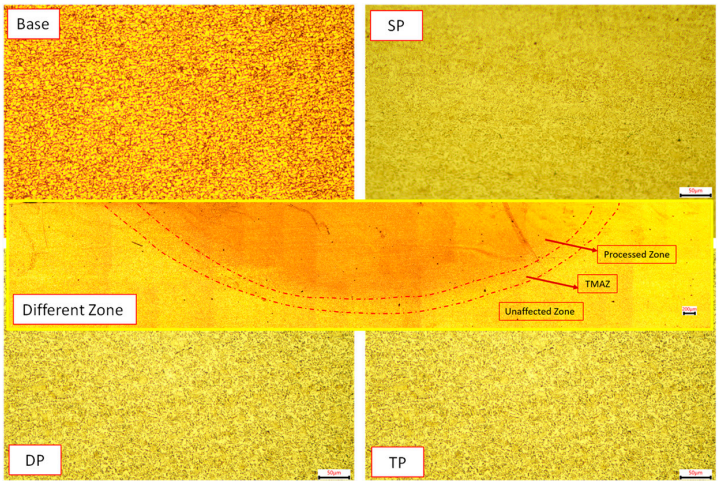

Figure 4. Optical micrographs of friction stir-processed samples after single, double, and triple passes.

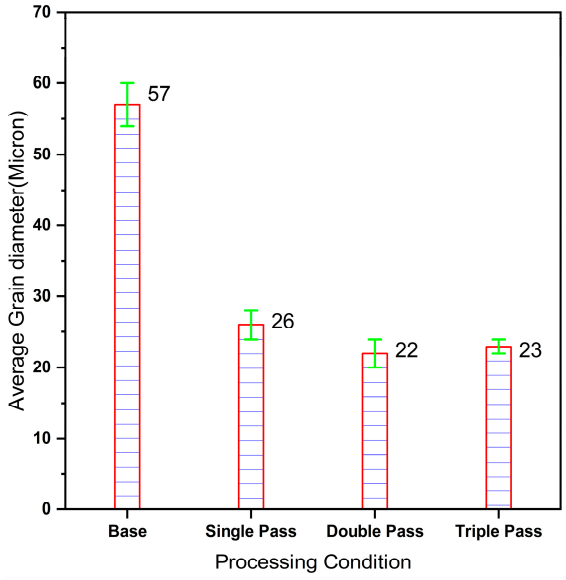

Figure 5. Average grain size of friction stir-processed samples after single, double, and triple passes.

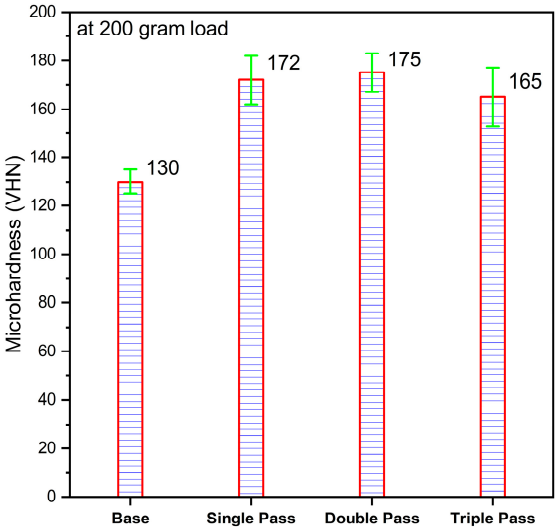

Figure 6. Measured microhardness of friction stir-processed samples after single, double, and triple passes.

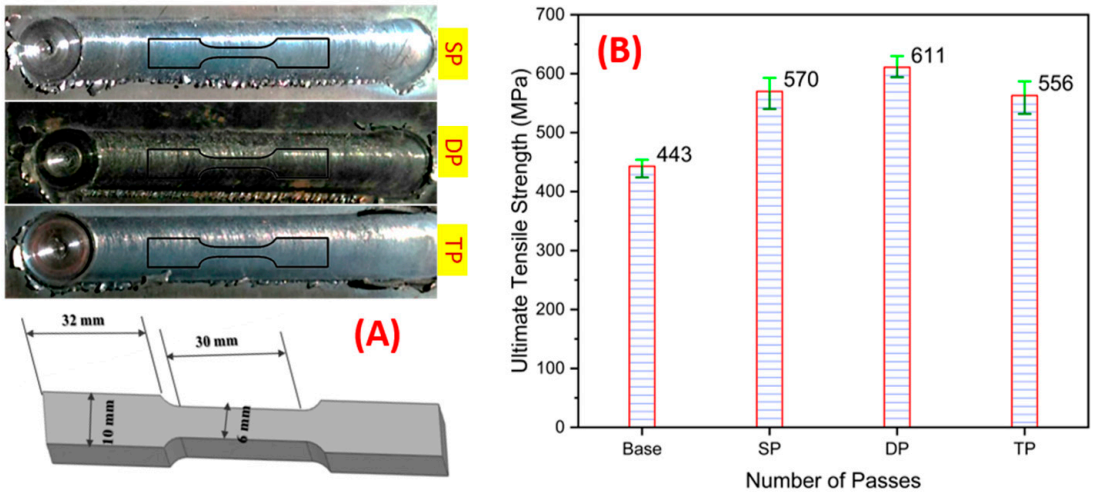

Figure 7. (**A**) Location of test specimen with dimensions. (**B**) Tensile strength of single pass-, double pass-, and triple pass-processed samples.

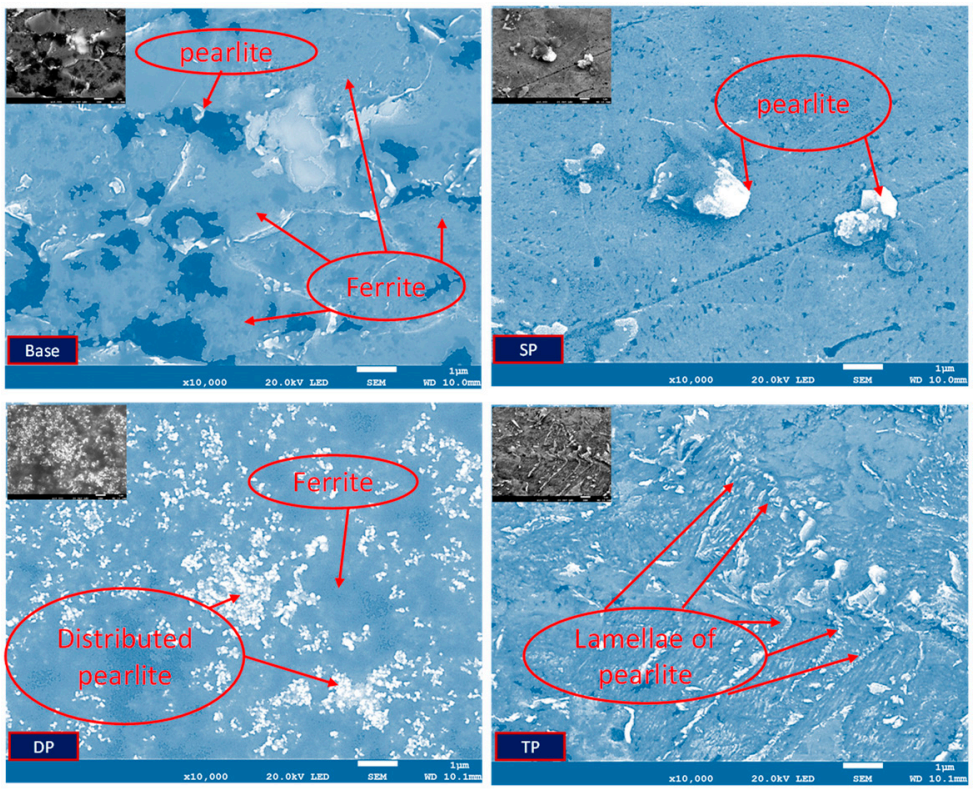

Figure 8. SEM image of friction stir-processed samples after single, double, and triple passes.

Figure 9 shows the EBSD image with high-angle and low-angle grain boundaries. High-angle grain boundaries are shown in a red color, whereas low-angle grain boundaries are represented using a green color.

Figure 10 shows the development of the crystallographic texture for the single pass, double pass, and triple pass specimens, in terms of their pole figures.

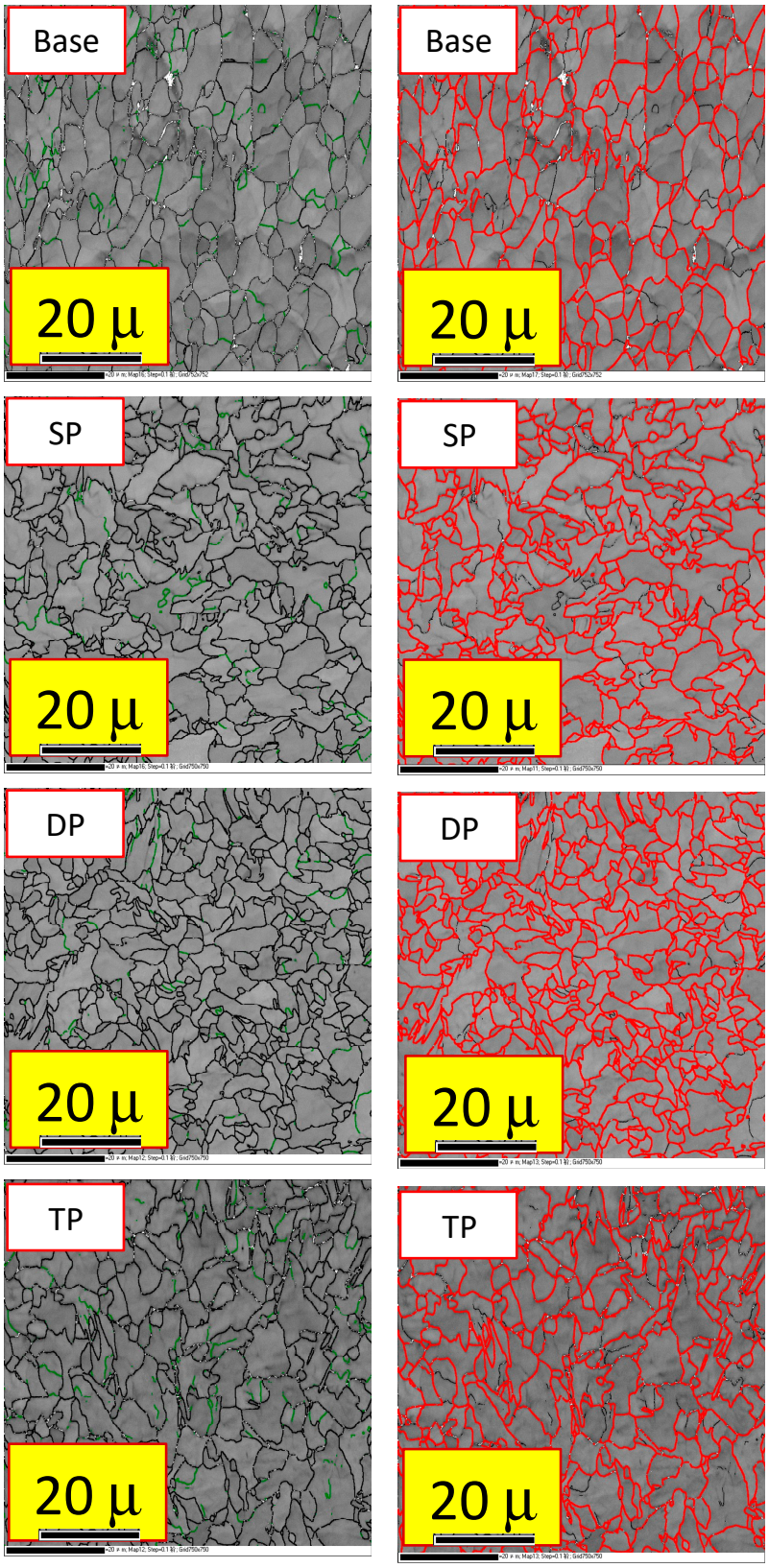

Figure 9. High-angle and low-angle grain boundaries of friction stir-processed samples after single, double, and triple passes.

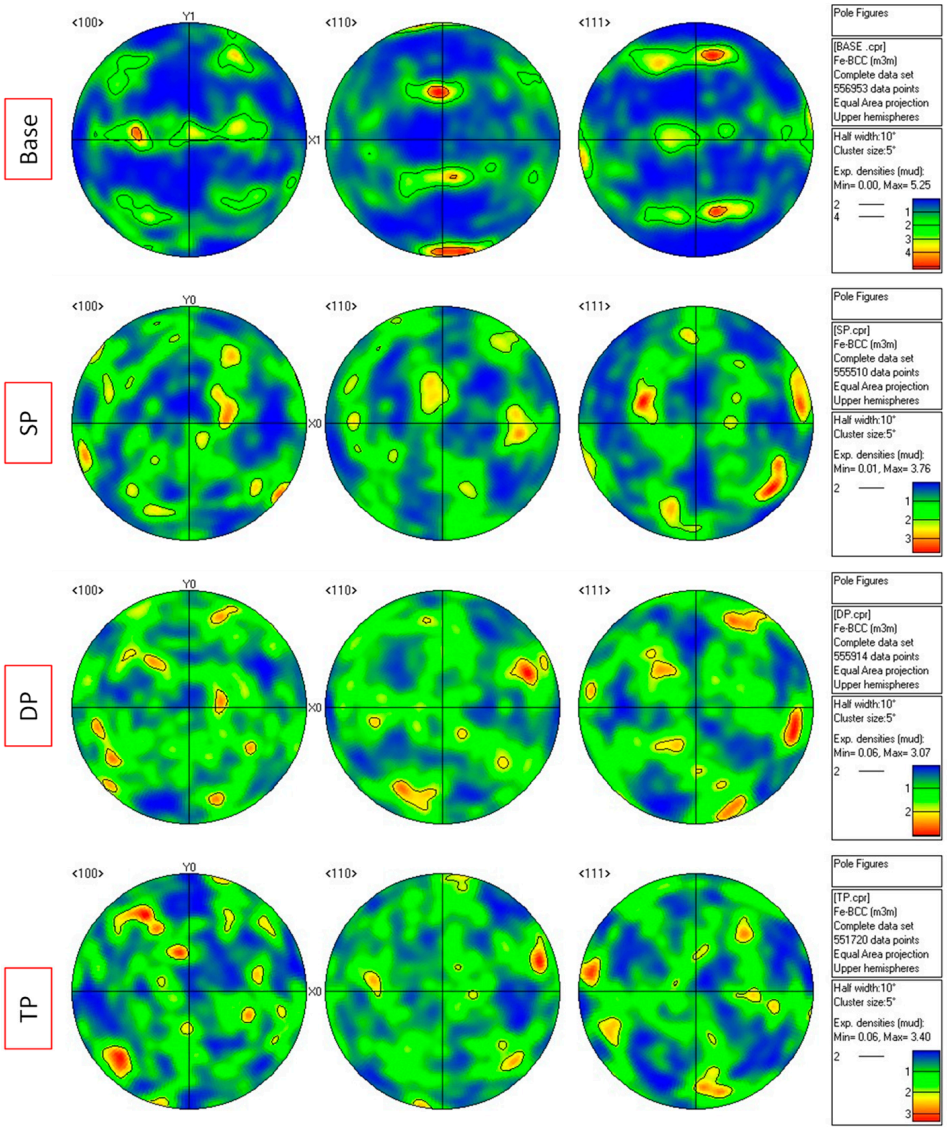

Figure 10. Crystallographic texture images of friction stir-processed samples after single, double, and triple passes.

4. Discussions

From Figure 3, it is clearly evident that the third pass altered the material properties up to a depth of 2.52 mm, in comparison to first pass of 2.21 mm, whereas the second pass processed up to 2.27 mm; the pin length was 2.20 mm for all the passes. The width of the processed zone also varied as the number of passes increased. The top of the nugget zone was measured as having a width of 11.27 mm after a triple pass, whereas a width of 11.17 mm was measured after the double pass, and a width of 9.99 mm was measured after a single pass, with the incorporation of a 10 mm shoulder diameter. This increase in depth and width with the number of passes can be attributed to an increase in the exposure time at elevated temperatures during FSP, and thus leads to an increase in the volumetric dimensions of the nugget zone on the third pass.

Stirring of the plasticized material at elevated temperate recrystallized the grains of the work materials. During the stirring of the materials, smaller grains were obtained due to a more even distribution of the grains. More even distributions of the grains will reduce the dislocation, hence allowing for a lesser deformation. A reduced amount of deformation will strengthen the work material. Smaller grains of the materials have a greater ration of surface area to volume of the materials, which leads to a greater ration of grain boundary

to dislocations. Hence, more force is required to break the elevated grain boundaries of the smaller grains. The double pass process allows for a more even distribution of grains, which may remain undistributed after a single pass. Hence, double pass processing evidences the smallest grains of 22 microns, on average. The most superior mechanical properties of the processed zone were achieved after a second pass of friction stir processing. The degree of grain refinement increased using double pass processing and, quite interestingly, the triple pass processing resulted in a little bit of grain coarsening, in comparison to double pass. The microstructure of the FSP sample clearly indicates approximately a two times smaller grain size in comparison to the as-received base material, as shown in Figure 5.

Grain refinement upon friction stir processing leads to the increased hardness of the processed sample, in comparison to the base metal hardness. The as-received IS2062 mild steel has an average hardness of 130 HV at a 200 g load, whereas a double pass of FSP increases the hardness value to 175 HV at the same load, as shown in Figure 6. The microhardness was taken from the center of processed zone for all cases.

The longitudinal center portion of the weld nugget was chosen to cut the tensile specimen of 100 mm in length. Double pass-processed samples revealed a UTS of 611 MPa, which is the highest among all the samples. Single pass-processed samples became fractured, with a UTS of 570 MPa, and triple pass-processed samples have a UTS of 556 MPa, whereas the as-received base material has a UTS of 443 MPa. All the results are shown in Figure 7.

During the processing, the used tungsten carbide tool becomes red hot, which advocates the peak temperature of around 1100 °C. This temperature allows for some growth of austenite grains in the nugget zone. During cooling, the generated austenite decomposed into fine grains of ferrite and pearlite, as clearly evidenced from the SEM image of the triple pass-processed samples (Figure 8). A triple pass of FSP exposed the maximum duration of the thermal cycle (heating and cooling). Due to this thermal cycle, Pearlite transformed into austenite during heating, whereas austenite transformed into pearlite during cooling. Hence, triple pass processing shows colonies of fine pearlite, along with a few ferrite grains.

The volume of high-angle grain boundaries is larger in all the processed samples due to the dynamic recrystallization, whereas the percentage of low-angle grain boundaries is lower, as a very low dynamic recovery has occurred. Among them, the second pass method of processing revealed the lowest volume of low-angle grain boundaries, as the rotating tool induces large grain rotations during the second pass of processing.

The base specimen manifests a weak rolling texture with the peak MUD (multiples of uniform distribution) lying around 5.25. With the increasing number of passes, the texture randomizes; however, the single and double pass methods indicate a higher randomization (MUD~3.07) in comparison to the subsequent passes. An MUD < 1 indicates the randomly oriented grains [37]. The continuous rotary motion of the tool induces large grain rotations near the high-angle grain boundaries, which act as nucleation sites for the Dynamically Recrystallized Grains (DRX). This combination results in a significant grain refinement in the microstructure (after a second pass), thus leading to an increase in texture randomization in comparison to the base material.

5. Conclusions

In the present work, the multi-pass friction stir processing of mild steel samples was successfully conducted. The following conclusions may be drawn from this experimental study:

1. Friction stir processing results in grain refinement in the friction stir-processed samples, from an average grain size of 57 microns to 22 microns after the second pass, due to the thermally associated plastic deformation of the material. The grain refinement in the processed region increases the microhardness of the processed sample in comparison to the base metal.
2. The surface properties of steel can be modified using friction stir processing due to the grain refinement and enhancement in microhardness; double pass friction stir process-

ing further refines the grain size up to 22 microns and increases the microhardness (175 VHN) in comparison to single pass (172 VHN). But triple pass processing causes a little bit of coarsening of the grains and a reduction in microhardness (165 VHN) in comparison to double pass processing.

3. The second pass-processed sample shows the maximum grain refinement due to the combined effects of large grain rotations and dynamic recrystallization near the high-angle grain boundaries.

Author Contributions: Conceptualization, H.S. and C.W.; methodology, A.R.R.; software, A.R.R.; validation, A.R.R., H.S. and C.W.; formal analysis, H.S.; investigation, A.R.R.; resources, C.W.; data curation, A.R.R.; writing—original draft preparation, A.R.R.; writing—review and editing, H.S. and C.W.; visualization, A.R.R.; supervision, C.W.; project administration, H.S. and C.W.; funding acquisition, C.W. All authors have read and agreed to the published version of the manuscript.

Funding: This research received no external funding.

Data Availability Statement: The raw data supporting the conclusions of this article will be made available by the authors on request.

Conflicts of Interest: The authors declare no conflicts of interest.

References

1. Mishra, R.S.; Ma, Z.Y. Friction Stir Welding and Processing. *Mater. Sci. Eng. R Rep.* **2005**, *50*, 1–78. [CrossRef]
2. Akbarpour, M.R.; Mirabad, H.M.; Gazani, F.; Khezri, I.; Ahmadi Chadegani, A.; Moeini, A.; Kim, H.S. An Overview of Friction Stir Processing of Cu–SiC Composites: Microstructural, Mechanical, Tribological, and Electrical Properties. *J. Mater. Res. Technol.* **2023**, *27*, 1317–1349. [CrossRef]
3. Gan, Y.X.; Solomon, D.; Reinbolt, M. Friction Stir Processing of Particle Reinforced Composite Materials. *Materials* **2010**, *3*, 329–350. [CrossRef]
4. Balasubramanian, N.; Mishra, R.S.; Krishnamurthy, K. Friction Stir Channeling: Characterization of the Channels. *J. Mater. Process. Technol.* **2009**, *209*, 3696–3704. [CrossRef]
5. Laska, A.; Sadeghi, B.; Sadeghian, B.; Taherizadeh, A.; Szkodo, M.; Cavaliere, P. Temperature Evolution, Material Flow, and Resulting Mechanical Properties as a Function of Tool Geometry during Friction Stir Welding of AA6082. *J. Mater. Eng. Perform.* **2023**, *32*, 10655–10668. [CrossRef]
6. Akbari, M.; Aliha, M.R.M.; Berto, F. Investigating the Role of Different Components of Friction Stir Welding Tools on the Generated Heat and Strain. *Forces Mech.* **2023**, *10*, 100166. [CrossRef]
7. Ma, X.; Xu, S.; Wang, F.; Zhao, Y.; Meng, X.; Xie, Y.; Wan, L.; Huang, Y. Effect of Temperature and Material Flow Gradients on Mechanical Performances of Friction Stir Welded AA6082-T6 Joints. *Materials* **2022**, *15*, 6579. [CrossRef] [PubMed]
8. Doude, H.R.; Schneider, J.A.; Nunes, A.C. Influence of the Tool Shoulder Contact Conditions on the Material Flow during Friction Stir Welding. *Metall. Mater. Trans. A Phys. Metall. Mater. Sci.* **2014**, *45*, 4411–4422. [CrossRef]
9. Wang, X.; Gao, Y.; Liu, X.; McDonnell, M.; Feng, Z. Tool-Workpiece Stick-Slip Conditions and Their Effects on Torque and Heat Generation Rate in the Friction Stir Welding. *Acta Mater.* **2021**, *213*, 116969. [CrossRef]
10. Heidarzadeh, A.; Mironov, S.; Kaibyshev, R.; Çam, G.; Simar, A.; Gerlich, A.; Khodabakhshi, F.; Mostafaei, A.; Field, D.P.; Robson, J.D.; et al. Friction Stir Welding/Processing of Metals and Alloys: A Comprehensive Review on Microstructural Evolution. *Prog. Mater. Sci.* **2021**, *117*, 100752. [CrossRef]
11. Prangnell, P.B.; Heason, C.P. Grain Structure Formation during Friction Stir Welding Observed by the "Stop Action Technique". *Acta Mater.* **2005**, *53*, 3179–3192. [CrossRef]
12. Saito, N.; Shigematsu, I.; Komaya, T.; Tamaki, T.; Yamauchi, G.; Nakamura, M. Grain Refinement of 1050 Aluminum Alloy by Friction Stir Processing. *J. Mater. Sci. Lett.* **2001**, *20*, 1913–1915. [CrossRef]
13. Mirshekari, B.; Zarei-Hanzaki, A.; Barabi, A.; Abedi, H.R.; Lee, S.J.; Fujii, H. An Anomalous Effect of Grain Refinement on Yield Stress in Friction Stir Processed Lightweight Steel. *Mater. Sci. Eng. A* **2021**, *799*, 140057. [CrossRef]
14. Patel, V.; Li, W.; Andersson, J.; Li, N. Enhancing Grain Refinement and Corrosion Behavior in AZ31B Magnesium Alloy via Stationary Shoulder Friction Stir Processing. *J. Mater. Res. Technol.* **2022**, *17*, 3150–3156. [CrossRef]
15. Xu, W.; Yu, J.; Jia, L.; Gao, C.; Miao, Z.; Wu, G.; Li, G.; Zhang, Z. Grain Refinement Impact on the Mechanical Properties and Wear Behavior of Mg-9Gd-3Y-2Zn-0.5Zr Alloy after Decreasing Temperature Reciprocating Upsetting-Extrusion. *J. Magnes. Alloys* **2022**, *10*, 3506–3519. [CrossRef]
16. Busu, N.; Jaffarullah, M.S.; Low, C.Y.; Shaari, M.S.B.; Armansyah; Jaffar, A. A Review of Force Control Techniques in Friction Stir Process. *Procedia Comput. Sci.* **2015**, *76*, 528–533. [CrossRef]

17. Wang, D.; Du, D.; Dong, A.; Li, J.; Toursangsaraki, M.; Sun, H. Investigations on Friction Stir Composite Processing and Picosecond Laser-Induced Surface Modification on Mechanical Properties of β-Titanium Alloy. *Mater. Today Commun.* **2024**, *38*, 108041. [CrossRef]
18. Alzahrani, M.A.; Alsoruji, G.; Moustafa, E.B.; Mosleh, A.O.; Mohamed, S.S. Optimization of Friction Stir Processing Parameters for Improvement of Mechanical Properties of $AlSi_7Mg_{0.2}$ Alloy. *Coatings* **2023**, *13*, 1667. [CrossRef]
19. Yue, S.; Huang, J.; Ni, Y.; Shen, L.; Huang, Y.; Fan, D.; Liu, J. Enhancing Microstructural, Mechanical, and Tribological Behavior of AZ31B Magnesium Alloy through Friction Stir Processing. *J. Mater. Res. Technol.* **2024**, *29*, 1441–1452. [CrossRef]
20. Sahu, P.K.; Singh, S.; Chen, G.; Yijun, L.; Zhang, S.; Shi, Q. Wear Behavior of the Friction Stir Alloyed AZ31 Mg at Different Volume Fractions of Al Particles Reinforcement and Its Enhanced Quality Attributes. *Tribol. Int.* **2020**, *146*, 106268. [CrossRef]
21. Khan, M.A.; Butola, R.; Gupta, N. A review of nanoparticle reinforced surface composites processed by friction stir processing. *J. Adhes. Sci. Technol.* **2023**, *37*, 565–601. [CrossRef]
22. Nascimento, F.; Santos, T.; Vilaça, P.; Miranda, R.M.; Quintino, L. Microstructural modification and ductility enhancement of surfaces modified by FSP in aluminium alloys. *Mater. Sci. Eng. A* **2009**, *506*, 16–22. [CrossRef]
23. Iwaszko, J.; Sajed, M. Technological aspects of producing surface composites by friction stir processing—A review. *J. Compos. Sci.* **2021**, *5*, 323. [CrossRef]
24. He, C.L.; Zhang, J.G.; Ren, C.Z.; Wang, S.Q.; Cao, Z.M. Characteristics of cutting force and surface finish in diamond turning of polycrystalline copper achieved by friction stir processing (FSP). *J. Mater. Process. Technol.* **2022**, *301*, 117451. [CrossRef]
25. Wang, W.; Han, P.; Peng, P.; Zhang, T.; Liu, Q.; Yuan, S.N.; Wang, K.S. Friction Stir Processing of Magnesium Alloys: A Review. *Acta Metall. Sin. (Engl. Lett.)* **2020**, *33*, 43–57. [CrossRef]
26. Ralls, A.M.; Kasar, A.K.; Menezes, P.L. Friction stir processing on the tribological, corrosion, and erosion properties of steel: A review. *J. Manuf. Mater. Process.* **2021**, *5*, 97. [CrossRef]
27. Eskandari, F.; Atapour, M.; Golozar, M.A.; Sadeghi, B.; Cavaliere, P. Corrosion behavior of friction stir processed AISI 430 ferritic stainless steel. *Mater. Res. Express.* **2019**, *6*, 086532. [CrossRef]
28. Ralls, A.M.; Daroonparvar, M.; Kasar, A.K.; Misra, M.; Menezes, P.L. Influence of friction stir processing on the friction, wear and corrosion mechanisms of solid-state additively manufactured 316L duplex stainless steel. *Tribol. Int.* **2023**, *178*, 108033. [CrossRef]
29. Abbasi, M.; Bagheri, B.; Dadaei, M.; Omidvar, H.R.; Rezaei, M. The effect of FSP on mechanical, tribological, and corrosion behavior of composite layer developed on magnesium AZ91 alloy surface. *Int. J. Adv. Manuf. Technol.* **2015**, *77*, 2051–2058. [CrossRef]
30. Niu, D.; Zhang, C.; Sui, X.; Lu, X.; Zhang, X.; Wang, C.; Shi, Z. Microstructure, mechanical properties and tribo-corrosion mechanism of $(CrNbTiAlVMo)_xN_{1-x}$ coated 316 L stainless steel in 3.5 wt% NaCl solution. *Tribol. Int.* **2022**, *173*, 107638. [CrossRef]
31. Han, J.; Chen, J.; Peng, L.; Tan, S.; Wu, Y.; Zheng, F.; Yi, H. Microstructure, Texture and Mechanical Properties of Friction Stir Processed Mg-14Gd Alloys. *Mater. Des.* **2017**, *130*, 90–102. [CrossRef]
32. Orozco-Caballero, A.; Ruano, O.A.; Rauch, E.F.; Carreño, F. Severe Friction Stir Processing of an Al-Zn-Mg-Cu Alloy: Misorientation and Its Influence on Superplasticity. *Mater. Des.* **2018**, *137*, 128–139. [CrossRef]
33. Miles, M.P.; Gunter, C.; Liu, F.; Nelson, T.W. Friction Stir Processing of 304L Stainless Steel for Crack Repair. In *Friction Stir Welding and Processing IX*; The Minerals, Metals & Materials Series; Springer: Cham, Switzerland, 2017; pp. 13–22. [CrossRef]
34. Selvam, K.; Mandal, P.; Grewal, H.S.; Arora, H.S. Ultrasonic Cavitation Erosion-Corrosion Behavior of Friction Stir Processed Stainless Steel. *Ultrason. Sonochem.* **2018**, *44*, 331–339. [CrossRef] [PubMed]
35. El-Sayed, M.M.; Shash, A.Y.; Abd-Rabou, M.; ElSherbiny, M.G. Welding and Processing of Metallic Materials by Using Friction Stir Technique: A Review. *J. Adv. Join. Process.* **2021**, *3*, 100059. [CrossRef]
36. *ASTM E-8*; Standard Test Methods for Tension Testing of Metallic Materials. ASTM International: West Conshohocken, PA, USA, 2020.
37. Bland, P.A.; Howard, L.E.; Prior, D.J.; Wheeler, J.; Hough, R.M.; Dyl, K.A. Earliest rock fabric formed in the Solar System preserved in a chondrule rim. *Nat. Geosci.* **2011**, *4*, 244–247. [CrossRef]

Disclaimer/Publisher's Note: The statements, opinions and data contained in all publications are solely those of the individual author(s) and contributor(s) and not of MDPI and/or the editor(s). MDPI and/or the editor(s) disclaim responsibility for any injury to people or property resulting from any ideas, methods, instructions or products referred to in the content.